Light Conversion by Electrochemiluminescence at Semiconductor Surfaces

Y. Zhao, J. Descamps, Yoan Léger, Neso Sojic, Gabriel Loget

Light Conversion by Electrochemiluminescence at Semiconductor Surfaces

Y. Zhao,[a] *J. Descamps,*[b] *Y. Léger,*[c] *N. Sojic,**[b] *G. Loget**[b]

[a] Univ Rennes, CNRS, ISCR (Institut des Sciences Chimiques de Rennes) – UMR 6226, Rennes 35000, France

[b] University of Bordeaux, Bordeaux INP, ISM, UMR CNRS 5255, Pessac 33607, France

[c] Univ Rennes, INSA Rennes, CNRS, Institut FOTON – UMR 6082, F-35000 Rennes, France

TOC GRAPHIC

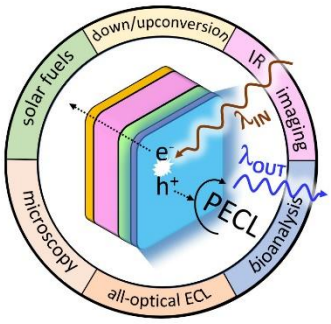

CONSPECTUS

Electrochemiluminescence (ECL) is the electrochemical generation of light. It involves an interfacial charge transfer that produces the excited state of a luminophore at an electrode surface. ECL is a powerful readout method that is widely employed for immunoassays and clinical diagnostics and is progressively evolving into a microscopy technique. On the other hand, photoelectrochemistry at illuminated semiconductors is a field of research that deals with the charge transfer of photogenerated charge carriers at the solid-liquid interface. This concept offers several advantages such as a considerable lowering of the onset potential required for triggering an electrochemical reaction as well as light addressable chemistry, *via* the spatial confinement of redox reactions at locally-illuminated semiconductor electrodes. The combination of ECL with photoelectrochemistry at illuminated semiconductors is referred to as photoinduced ECL (PECL). It deals with the triggering of an ECL reaction through the transfer of photogenerated minority charge carriers at the illuminated solid/liquid interface. PECL results in the conversion of incident photons (λ_{exc}), that are absorbed by the semiconductor photoelectrode to emitted photons (λ_{PECL}), produced by the ECL reaction. Although demonstrated in the seventies by Bard *et al.* in ultradry organic solvents, PECL remained unexplored until the last five years. Nowadays, as a result of the considerable progress achieved in semiconductor photoelectrodes and ECL systems, a large variety of PECL systems can be designed by combining photoelectrode materials with ECL luminophores, making it a versatile tool for light conversion in aqueous media. In this Account, we introduce the fundamentals of ECL and photoelectrochemistry at illuminated semiconductors and review the recent developments in PECL. We discuss the two main PECL light conversion schemes: downconversion (where $\lambda_{exc} < \lambda_{PECL}$) and upconversion (where $\lambda_{exc} > \lambda_{PECL}$). Besides, PECL can

be used to simplify considerably the common electrochemical setups employed for ECL. Indeed, by engineering the photoelectrode material and carefully considering the reactivity involved for ECL and its counter-reaction, PECL enables the ultimate concept of all-optical ECL (AO-ECL), i.e., ECL generation at an illuminated monolithic device immersed into the electrolyte solution. As discussed in this Account, AO-ECL is an important breakthrough that allows the simplest ECL experimental configuration ever reported, eliminating constraints such as electrical power supply, wires, electrodes, connections, and specific electrochemical knowledge. As shown at the end of this Account, due to the robustness of recently manufactured PECL systems, several applications can already be envisioned for microscopy, elucidation of mechanisms solar conversion mechanisms, near-infrared imaging, and bioanalysis.

KEY REFERENCES

- Zhao, Y.; Yu, J.; Xu, G.; Sojic, N.; Loget, G. Photoinduced electrochemiluminescence at silicon electrodes in water. *J. Am. Chem. Soc.* **2019**, 141 (33), 13013–13016.[1] First demonstration of photoinduced ECL (PECL) in water.

- Zhao, Y.; Descamps, J.; Ababou-Girard, S.; Bergamini, J.-F.; Santinacci, L.; Léger, Y.; Sojic, N.; Loget, G. Metal-insulator-semiconductor anodes for ultrastable and site-selective upconversion photoinduced electrochemiluminescence. *Angew. Chem. Int. Ed.* **2022**, 61 (20), e2022018.[2] Considerable improvement in the stability of PECL.

- Zhao, Y.; Descamps, J.; Hoda Al Bast, N.; Duque, M.; Esteve, J.; Sepulveda, B.; Loget, G.; Sojic, N. All-optical electrochemiluminescence. *J. Am. Chem. Soc.* **2023**, 145, 17420–17426.[3] First demonstration of all-optical ECL (AO-ECL).

- Descamps, J.; Zhao, Y.; Goudeau, B.; Manojlovic, D.; Loget, G.; Sojic, N. Infrared photoinduced electrochemiluminescence microscopy of single cells. *Chem. Sci.* **2024**, 15, 2055–2061.[4] Application of PECL to the microscopy characterization of cells.

1. INTRODUCTION

1.1. Electrochemiluminescence

Electrochemiluminescence (ECL), or "electrogenerated chemiluminescence", is the light emission resulting from an initial electrochemical reaction occurring at an electrode surface.[5] Nowadays, ECL is mainly based on the reaction of a luminophore with a sacrificial co-reactant in aqueous electrolytes. The excited state of the luminophore is produced by the very exergonic electron-transfer reaction between the electrogenerated species or by a bond-breaking reaction. Then, it spontaneously relaxes to its ground state by emitting a photon (λ_{ECL}).[6] The most efficient and widely used ECL system is composed of the tris(bipyridine) ruthenium(II) luminophore ($[Ru(bpy)_3]^{2+}$ and the sacrificial tri-*n*-propylamine (TPrA) co-reactant that yields a red emission (λ_{ECL} = 620 nm) in aqueous media. Another model system is luminol with hydrogen peroxide that produces blue light (λ_{ECL} = 425 nm) in an alkaline aqueous solution. A particularity of the ECL light is that the local emission at the electrode surface occurs within a few-micrometer-thick layer without requiring an incident light, leading to a luminescence signal with a near-zero background.[7] ECL is mainly applied in (bio)analytical applications such as clinical tests or immunoassays,[8,9] and has also extended to microscopy and bioimaging.[10–14] Two main ECL imaging configurations have been developed by playing differently with light and darkness: *i*) positive ECL: a bright object (ECL-active or labeled entity) emitting ECL on a dark background (i.e. bare electrode) and *ii*) negative label-free ECL: a dark object (typically, a living cell) surrounded by a bright background[15,16] (i.e. bare electrode). Two disadvantages of ECL, which are addressed by PECL, are the relatively complex required experimental setup and the fact all the immersed conductive electrode area is active.

1.2. Photoelectrochemistry at semiconductor surfaces

Although discovered in 1839,[17] the report by Fujishima and Honda on photoelectrochemical water electrolysis sparked the popularity of photoelectrochemistry (PEC) at semiconductors (SCs).[18] Generally speaking, PEC at SCs is a field of research that studies light-absorbing SC-based photoactive electrodes (photoelectrodes) immersed in an electrolyte. A typical photoelectrode comprises a depletion layer.[19,20] Upon absorption of incident photons with an energy higher than the SC bandgap, minority charge carriers reaching the depletion layer (*e.g.*, holes (h^+) in the case of an *n*-type SC photoanode) can trigger an electrochemical reaction at the SC/electrolyte interface. This situation generally results in the creation of a photovoltage (V_{OC}) in the SC which induces a decrease in the potential required to trigger the electrochemical reactions under illumination (i.e., a cathodic shift in the case of a photoanode). The field of PEC at SC has been widely developed in the frame of solar energy conversion, we refer the interested reader to Memming's excellent book.[21] Photoelectrodes can be based on SC/liquid, SC/SC[22] (e.g., in a *p-n* junction), or SC/metal junctions[23] (i.e., a Schottky junction). Unlike conventional PEC, PECL offers the possibility of an optical output of electrochemical processes and a unique access of local scale information.

2. PHOTOINDUCED ELECTROCHEMILUMINESCENCE

Photoinduced ECL (PECL) is a category of ECL that is triggered at an illuminated semiconductor interface.[24] It was originally proposed by *Bard et al.* in the seventies.[25,26] As shown in **Figure 1a,c**, in PECL, the semiconductor electrode produces charge carriers (i.e. h^+ or e^-) under illumination with incident light (λ_{exc}). Photogenerated minority carriers drive the ECL reaction in the liquid phase, thereby producing photons at another wavelength (λ_{PECL}).[2,27–30] In

these conditions, photogenerated minority carriers (i.e. h^+ or e^-) drive the ECL reaction with a lower overpotential than that of a non-photoactive electrode.[2,29] Depending on the illumination conditions, PECL is emitted homogeneously over the entire electrode area or localized on the electrode by focusing the incident light spot.[2] PECL can follow a downconversion type (with $\lambda_{PECL} > \lambda_{exc}$)[27,28] or upconversion type (with $\lambda_{PECL} < \lambda_{exc}$)[2,29,30] scheme depending on the experimental parameters.

2.1. Downconversion photoinduced electrochemiluminescence

Downconversion PECL was investigated at *n*-type metal oxides in water, as shown in **Figure 1a**. These SCs usually have better stability than narrow bandgap SCs and many of them have been widely studied in the frame of photoelectrochemical water splitting. Because of their wide bandgap, they can only absorb high-energy photons. In the two reported studies,[2,30] the downconversion PECL of a luminol analog, 8-amino-5-chloro-2,3-dihydro-7-phenyl-pyrido[3,4-d]pyri-dazine-1,4-dione (L-012) was studied in an alkaline electrolyte. The first example of downconversion PECL employed $BiVO_4$ as a photoanode, a *n*-SC having a bandgap of 2.4 eV. Ultraviolet (UV) illumination (λ_{exc} = 375 nm) was employed for excitation, a wavelength at which L-012 also absorbs and produces fluorescence (FL) (**Figure 1b**). The electrode was illuminated from the air/SiO_2/FTO interface (backside illumination), which led to L-012 FL at open circuit conditions. When the potential is applied to a value where L-012 is oxidized under illumination, PECL occurs, which induces the amplification of the overall luminescence (FL + PECL, **Figure 1a**). Due to the high V_{OC} and the low oxidation potential of L-012, in this work, PECL was generated at a potential as low as -0.4 V vs Ag/AgCl. Usually, anodic potentials of ~0.2V are required on non-photoactive electrodes. The downconversion PECL emission was dependent on the applied potential, the illumination intensity, and stable for ≈2 h. This PECL

mechanism was also tested on nanostructured hematite (α-Fe_2O_3) nanorod arrays.[28] Compared to $BiVO_4$, on this photoanode, PECL could be generated at a more positive potential of -0.2 V vs Ag/AgCl and a degradation of the PECL intensity was recorded during prolonged operation.

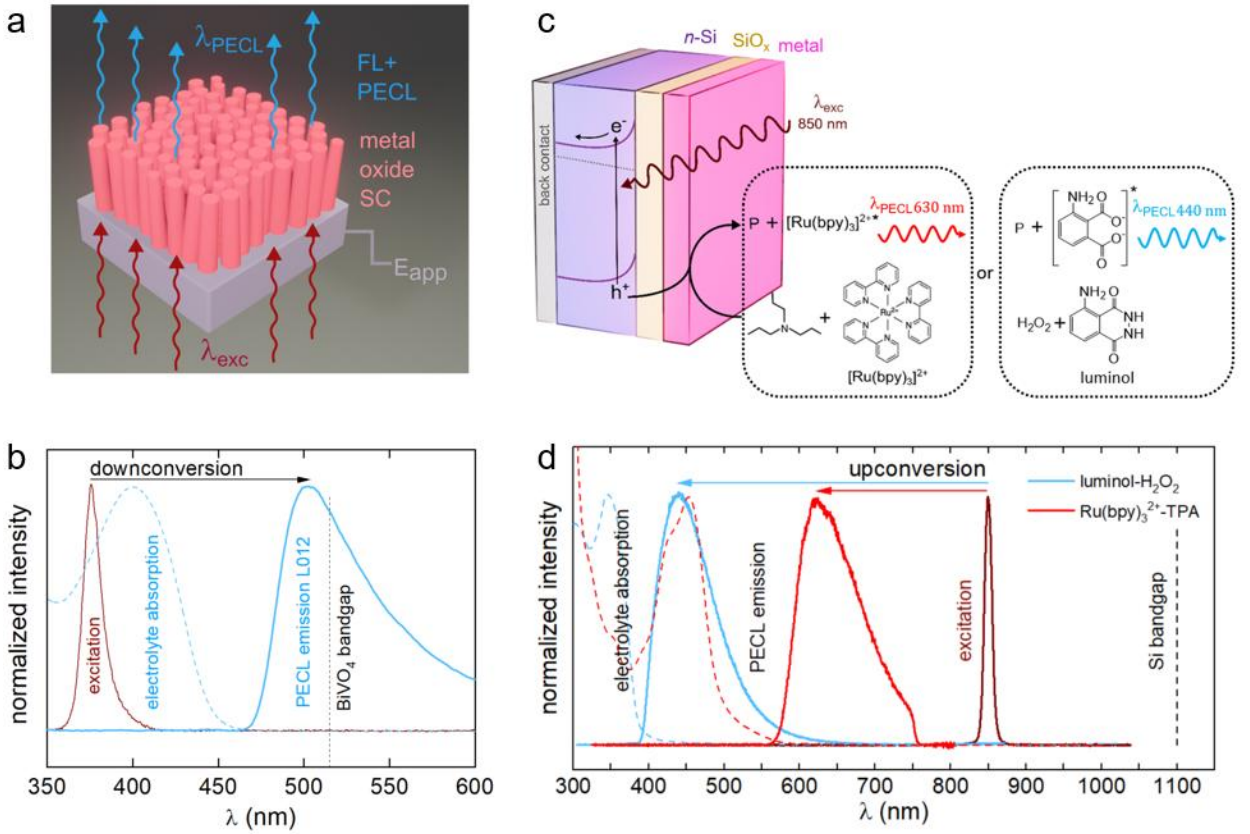

Figure 1. Down- and upconversion PECL. a) Luminescence amplification principle based on the generation of downconversion PECL. Adapted with permission from [28]. Copyright 2021 Elsevier. b) Normalized spectra showing the emission of the excitation source (brown curve), L-012 absorption (dashed blue curve), and emission of L-012 (plain line blue curve). Adapted with permission from [27]. Copyright 2020 Wiley. c) Scheme showing the photoinduced charge transfer process occurring at a MIS photoanode by upconversion PECL with $([Ru(bpy)_3]^{2+}$-TPrA or luminol-H_2O_2. Adapted with permission from [2]. Copyright 2022 Wiley. d) Normalized spectra, for $[Ru(bpy)_3]^{2+}$-TPrA (red curves) and luminol-H_2O_2 (blue curves), of the electrolyte absorption (dashed curves), emission of the NIR LED (brown curve), the PECL emission (full line curves).

2.2. Upconversion photoinduced electrochemiluminescence

In upconversion PECL, the absorption of low-energy photons by the photoelectrode generates minority carriers that cumulate energy from photogeneration and external potential. They can thus react with the ECL reactant and lead to higher-energy photons through the ECL reaction (**Figure 1c**). The first evidence for upconversion PECL was reported in the mid-seventies,[25,31] at the surface of narrow bandgap photocathodes (*p*-Si, *p*-InP, and *p*-GaAs) illuminated with near-infrared (NIR) light (λ_{exc} = 729 nm). The luminophore was 9,10-dichloro-9,10-dihydro-9,10-diphenyl-anthracene ($DPACl_2$) dissolved in acetonitrile. Upon electrochemical reduction, the anion radical $DPA^{\bullet-}$ chemically reacts with an intermediate to generate the DPA-excited singlet that emits at 413 nm. A more "conventional" way to trigger annihilation PECL is to generate the anion radical and the cation radical by applying a squarewave signal with anodic and cathodic pulses. This route was explored for *p*- and *n*-type InP and GaAs illuminated above 729 nm with a series of organic compounds in acetonitrile.[26] However, the stability of these mentioned SCs in such electrolytes was strongly limited. The recent progress in SC photoelectrode stabilization, achieved in the last years in the frame of the development of photoelectrochemical water splitting[23,32] allowed the current development of PECL systems that can operate in aqueous media, enabling PECL with modern co-reactant systems. In the following, we review the recent upconversion PECL examples achieved on Si-based photoelectrodes in aqueous electrolytes.[2,29,30] Because of its narrow bandgap of 1.12 eV Si can harvest photons from UV to NIR,[33] however due to its low stability (passivation during anodic reactions) and its weak electrocatalytic activity, a protective layer and a catalytic layer (or one layer with both properties) ought to be deposited on Si photoelectrodes to generate reactions with high efficiency and stability. Vogel *et al.* reported on the PECL of luminol-H_2O_2 at *n*-Si photoanodes covalently modified with protecting 1,8-nonadiyne monolayers for the conversion of λ_{exc} = 625 nm in λ_{PECL}

= 430 nm.[34] Our group showed that a thin metal (M) film with a thickness in the nanometer range sputtered onto a chemically oxidized Si surface (Si/SiO_x) preserves the electroactivity of Si immersed in aqueous ECL electrolytes. This sequence of materials ($Si/SiO_x/M$), shown in **Figure 1c**, is a variant of the well-known Schottky junction and is referred to as a metal/insulator/semiconductor (MIS) electrode. MIS electrodes can be used for ECL (in the case of highly-doped degenerate p^{++}-Si) or PECL (in the case of moderately doped and photoactive *n*-Si) with the anodic $[Ru(bpy)_3]^{2+}$-TPrA co-reactant system (see **Section 1.1.**).[2,29] In 2019, the first example of upconversion PECL in an aqueous electrolyte was reported with NIR incident light (λ_{exc} = 810 nm, λ_{PECL} = 635 nm with $[Ru(bpy)_3]^{2+}$-TPrA electrolyte) based on *n*-Si/SiO_x/Ni electrodes. It was observed that *n*-Si/SiO_x/Ni was inactive in the dark, however, when illuminated with NIR light, it afforded considerable photocurrent and PECL emission. The operation of this photoanode was demonstrated for 15 min with galvanostatic control under NIR light. In 2022, two other metals (Pt and Ir) were investigated and they increased the stability of the MIS electrodes in the $[Ru(bpy)_3]^{2+}$-TPrA ECL system. These metals are known for their good electrocatalytic activities and, according to their Pourbaix diagrams, higher stability[35] was expected in PECL conditions (pH = 7.4) than the previously used Ni thin films. As *n*-Si/SiO_x/Ni, both *n*-Si/SiO_x/Pt and *n*-Si/SiO_x/Ir were inactive in the dark and triggered PECL (λ_{PECL} = 630 nm) under NIR light (λ_{exc} = 850 nm). Subtraction of the onset potential values of ECL (p^{++}-Si/SiO_x/M in the dark) with that of PECL (illuminated *n*-Si/SiO_x/M) gives V_{OC} values of 485 and 280 mV for *n*-Si/SiO_x/Pt and *n*-Si/SiO_x/Ir photoanodes, respectively. V_{OC} values are correlated with the Schottky barrier height of the MIS device, which is theoretically controlled by the workfunction of the metal.[36] Among these 3 metals (Ni, Pt and Ir), Pt produces the highest Schottky barrier, which is explained by its highest workfunction. Long-term PECL stability was

assessed by galvanostatic experiments under homogeneous NIR illumination and the anode potential and PECL intensity were monitored. *n*-Si/SiO_x/Pt presented a potential below 2 V for 140 min and comparatively, *n*-Si/SiO_x/Ir exhibited exceptional stability and generated strong PECL over 35 h of operation with a minimal potential increase. These results were remarkable when considering the modest stability of *n*-Si/SiO_x/Ni (achieving an operation time for upconversion PECL of only 15 min). These performances are explained by the fact that during operation Pt and Ir remained mainly in the solid phase while Ni slowly dissolved in the neutral pH solution required for the $[Ru(bpy)_3]^{2+}$-TPrA ECL system. Another strategy was implemented to prevent Ni dissolution, that is, the use of an alkaline ECL system. For instance, luminol-H_2O_2, typically employed in 0.1 M KOH or NaOH solutions (see **Section 1.1.**).[30] At this pH, Ni is expected to be anodically stable, with the formation of an insoluble $Ni(OH)_2$ phase, which would likely remain on the *n*-Si substrate and increase its workfunction.[37] Other benefits of this system are that it emits at a shorter wavelength ($\lambda_{PECL} \approx 440$ nm) compared to $[Ru(bpy)_3]^{2+}$-TPrA ($\lambda_{PECL} \approx 630$ nm), allowing for larger anti-Stokes shifts (**Figure 1d**) and with a much lower emission onset potential. We note that upconversion PECL can also be generated with co-reactant systems at *p*-Si-based photocathodes,[38] which may open the door to new robust PECL photoelectrode operating through reduction reactions.

The PECL systems discussed above rely on wire-connected SC electrodes, on which a potential is directly applied. To get rid of wire connection, wireless PECL systems were first studied in bipolar electrochemical cells, where two external feeder electrodes connected to a power supply are located in the solution on either side of the Si bipolar electrode (BPE), without a direct contact.[39,40] At a sufficiently high potential drop in solution and under NIR illumination on the depleted pole, oxidation and reduction took place simultaneously at the poles of the Si BPE.

Closed BPEs based on photoactive *p*- or *n*-Si can be used further for the wireless generation of upconversion PECL under NIR illumination with bright emissions in the visible spectrum (with $[Ru(bpy)_3]^{2+}$-TPrA or with the L-012 system). The protection of the anodic pole of the Si BPE with a SiO_x/Ir coating provides stability to the BPE, which can operate for a long time (> 20 h) under NIR illumination. However, this bipolar PECL configuration still requires a power supply to polarize the feeder electrodes.

3. ALL-OPTICAL ELECTROCHEMILUMINESCENCE

All-optical ECL (AO-ECL) refers to wireless PECL systems that operate without an external power source. AO-ECL was inspired by research on monolithic water-splitting photoelectrochemical devices and can be considered as pushing and overcoming the limits of the PECL to create a new electrically-autonomous strategy.[18,41–46] In the reported AO-ECL systems,[3,47,48] which are based on Si, photogenerated holes and electrons trigger simultaneously the oxidative emission of visible ECL photons and the reduction of an oxidant present in solution, respectively. This can occur only if V_{OC} (see **Section 1.2.**), generated by the photovoltaic junction, is higher than the overpotential required for triggering both the ECL oxidation and the cathodic counter-reduction.

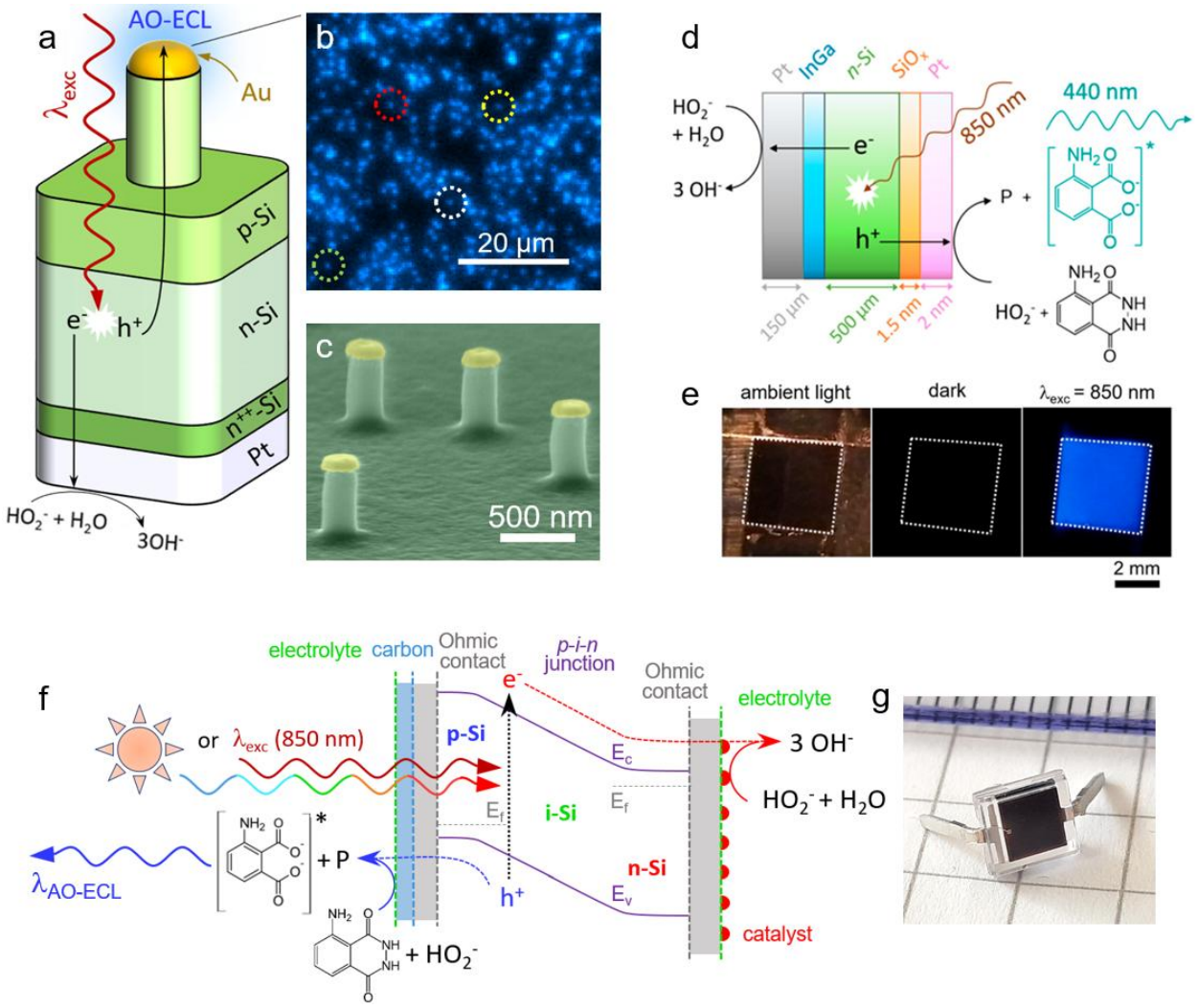

Figure 2. AO-ECL at various photoactive junctions. a) Scheme of monolithic AO-ECL at a nanostructured Au-*pnn*$^{++}$Si-Pt junction. b) Optical microscopy images of the Au-*pnn*$^{++}$Si-Pt frontside under NIR illumination. c) Colored SEM image showing the Au-*pnn*$^{++}$Si-Pt frontside. Adapted with permission from [3]. Copyright 2023 American Chemical Society. d) Scheme of AO-ECL emission at Pt/InGa/*n*-Si/SiO_x/Pt. e) Smartphone photographs showing the frontside of Pt/InGa/*n*-Si/SiO_x/Pt immersed in the electrolyte under ambient light (left), in the dark (middle) and near-IR illumination (right). Adapted with permission from [48]. Copyright 2024 American Chemical Society. f) Band diagram of a *pin* Si photodiode interfaced with a carbon and a catalyst layer, immersed in the ECL electrolyte. g) Photograph of a *pin* Si photodiode. Adapted with permission from [47]. Copyright 2024 Wiley.

Specific Si junctions were investigated. Besides material considerations, an important strategy for promoting AO-ECL is to select an electrolyte enabling high reactivity at low overpotentials in oxidation and in reduction. In this respect, the anodic luminol-H_2O_2 ECL system is

particularly adapted as it is known to allow PECL at low anodic overpotentials.[30,34] In addition, it contains H_2O_2, which is not only the ECL co-reactant (essential to promote emission) but can also be reduced at low cathodic overpotentials on appropriate metal catalysts.[49]

As shown in **Figure 2a**, AO-ECL was first reported with a nanostructured *pnn*$^{++}$Si photovoltaic junction, modified with catalytic Au and Pt coatings at each side of the device. Both coatings are required to trigger both anodic ECL reaction and the associated cathodic counter-reaction under illumination with a NIR LED (λ_{exc} = 850 nm). The frontside (i.e. the illuminated side) of the device comprised an array of randomly distributed Si nanopillars capped with Au nanodisks (**Figure 2c**). The electrochemical properties of the frontside (the Au-*pnn*$^{++}$Si photoanode) and the backside (the Pt cathode) were independently investigated in the presence of the ECL electrolyte by photoelectrochemical methods. This device generated a V_{OC} of 460 mV, revealing the possibility of the spontaneous AO-ECL. When the Au/*pnn*$^{++}$Si/Pt monolithic device was studied by immersing the entire surface in a transparent cell, under NIR light, intense blue AO-ECL was recorded with a smartphone camera. AO-ECL was observed only when NIR was applied at the device frontside and the emission signal responded instantaneously to the NIR stimulus. The emission intensity depended on the applied illumination power density and the H_2O_2 concentration and was stable for 30 min of operation. To identify precisely the location of the AO-ECL emission, the photoanodic face of the electrode was observed with an optical microscope. It revealed that the discrete AO-ECL spots colocalized with the position of the Au nanodisks located on the top of the nanopillars (**Figure 2b**). Then, a second AO-ECL device was developed, based on luminol-H_2O_2 ECL system and a simple Si Schottky junction.[48] The cathode, Pt/InGa/*n*-Si, was made by forming an Ohmic contact between Si and Pt and the photoactive Schottky anode was a MIS *n*-Si/SiO_x/Pt construct, as presented in **Figure 2d,e**.

Besides the effects of the illumination power density and H_2O_2 concentration, dissolved O_2 in the electrolyte also influenced AO-ECL on the Pt/InGa/*n*-Si/SiO_x/Pt device.[50] These results show that a simple Schottky-type Si-based PV junction can trigger AO-ECL, this is interesting because these junctions can be easily manufactured without the requirement of expensive equipment. The third PV junctions that has been studied for AO-ECL is a commercial *pin* Si junction (1 € $unit^{-1}$), which is a variant of the well-known *pn* junction in which an intrinsic layer (*i*-layer) is located between the *p*-type and the *n*-type layers. Since commercial *pin* junctions (usually employed as photodiodes, **Figure 2g**) are shielded within an insulating matrix, the only conductive surfaces that can promote solid/liquid charge transfer are the two conductive Sn-coated leads. Sn is a metal subject to anodic degradation at high pH,[35] which, in addition, has poor electrocatalytic activity for H_2O_2 reduction. To overcome these limitations, carbon was painted on the anode due to its well-established optimal ECL properties[51] and Pt was deposited on the cathode due to its efficient electrocatalytic activity for H_2O_2 oxidation. The *pin* photodiode produces V_{OC} values ranging from 0.45 to 0.53 V at different illumination power densities (λ_{exc} = 850 nm, 2.5 < P_{LED} < 18 mW cm^{-2}). Since a bias of 0.27 V is required to generate the ECL reaction and H_2O_2 reduction (**Figure 2f**) on a carbon anode and a Pt cathode, respectively, the *pin* photodiode is suitable to trigger intense AO-ECL. This last approach demonstrates the possibility to generate AO-ECL with cheap elements without the need of nanofabrication process and it could lead a wide range of applications in (bio)analytical disposable devices.

4. APPLICATIONS

4.1. Investigation of energy conversion mechanisms

The development of stable and bright PECL systems (**Section 2.2.**) opened the door for several applications. For instance, PECL has the potential for the investigation of heterogeneous charge

transfer mechanisms occurring on photoelectrodes designed for energy applications (e.g. artificial photosynthesis).[52] Indeed, PECL corresponds to a light signal emitted by a local charge transfer at the SC/electrolyte junction, which can reveal the local photoelectrochemical activity on heterogeneous and nanostructured photoelectrodes.[53,54] This potential application has been highlighted in a recent report where photoanodes based on *n*-Si/SiO_x were designed by depositing Ir (thickness ~3 nm) with different widths and pitchs.[55] PECL was triggered by a homogeneous illumination of the entire photoanode from a NIR LED (λ_{exc} = 850 nm) and was observed through an optical microscope with the $[Ru(bpy)_3]^{2+}$-TPrA system. The red light emitted by the $[Ru(bpy)_3]^{2+}$ (λ_{PECL} = 620 nm) was detected by a camera, suppressing the NIR light with a filter. The conductive Ir patterns appeared homogeneously for at least 30 min by PECL and the Ir-free Si surface passivated with SiO_x remained dark. The accuracy of the patterns detected by PECL was studied by comparing the PECL imaging to the SEM images, revealing a good correlation between both techniques. In addition, PECL microscopy has been reported by Xue *et al.* to image the plasmonic photoelectrochemistry activity of single nanocatalysts, as shown in **Figure 3a,b**.[56] Under laser irradiation, single Au nanoparticles (Au NPs) deposited on TiO_2 produced photogenerated hot holes at their surface, which oxidized L-012 and induced blue PECL emission. The authors found that the emitted ECL density on single AuNPs decreased with an increase in particle diameter. These remarkable results demonstrated the possibility of mapping the catalytic activity of single photocatalysts by PECL microscopy.

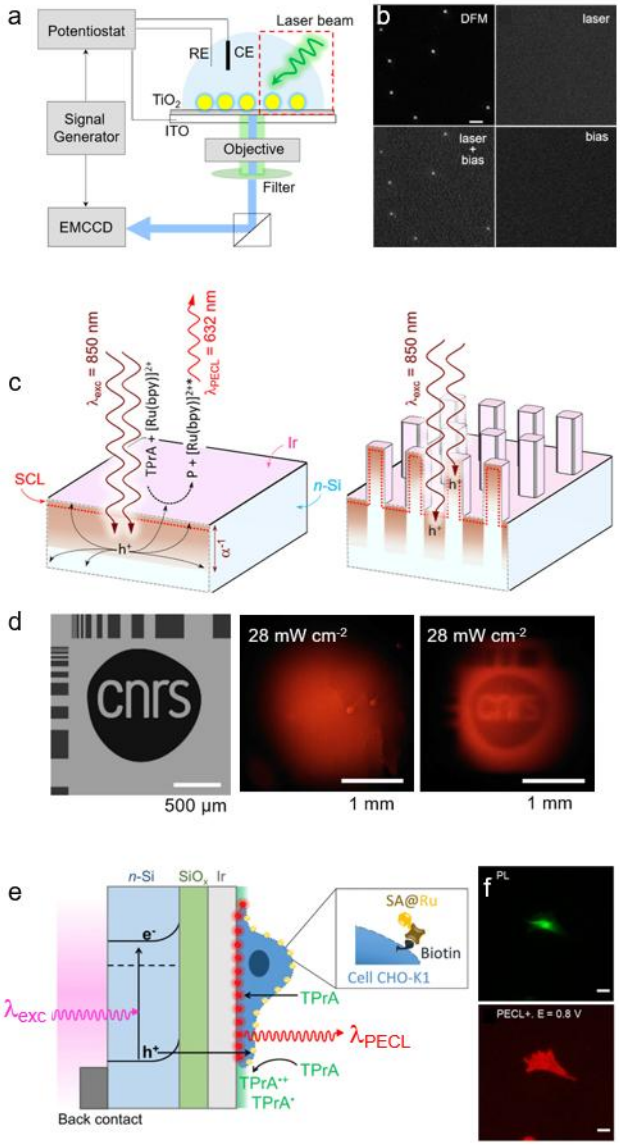

Figure 3. Applications of PECL. a) Schematic illustration of the ECL imaging of plasmonic photocatalysis at single AuNPs on TiO_2. b) Dark-field microscopy (DFM), image recorded under 532 nm laser irradiation, PECL image and image recorded with a bias of 0.6 V of 200 nm AuNPs deposited on TiO_2. Adapted with permission from [56]. Copyright 2023 American Chemical Society. c) Sketches showing the generation and diffusion of holes within planar *n*-Si/SiO_x/Ir (left panel) and microstructured *n*-Si/SiO_x/Ir (right panel) photoanodes during PECL emission. d) NIR pattern projected on the photoanode (left panel), corresponding PECL images recorded on planar *n*-Si_{plan}/SiO_x/Ir (middle panel) and microstructured *n*-SiMPs/SiO_x/Ir (right panel). Adapted with permission from [57]. Copyright 2024 American Chemical Society. e) Direct imaging by positive PECL of cell membrane labeled with streptavidin-modified $[Ru(bpy)_3]^{2+}$ luminophore (SA@Ru) in TPrA solution. f) Photoluminescence (PL) micrograph (top panel,

green color) and positive PECL images (bottom panel, red color) of cells labeled with SA@Ru. Adapted with permission from [4]. Copyright 2024 Royal Society of Chemistry.

4.2. NIR imaging

As reported in previous work, the use of a focused excitation light yields local PECL emission.[2,25,34] Therefore, PECL can also be used for NIR imaging and can transform a NIR image, invisible to the human eye, into a visible image. The reported PECL-based NIR imaging method involves $[Ru(bpy)_3]^{2+}$-TPrA ECL system and a Si-based MIS photoanode.[57] Localized PECL was first studied on a biased planar *n*-Si/SiO_x/Ir photoanode under the irradiation with a 60-µm NIR wide laser beam and a 230-µm wide PECL spot was measured. Although it was evident that PECL was generally emitted in correspondence with the illuminated area, the resolution was very low. This is not surprising due to the long lateral diffusion of photogenerated carriers in crystalline Si, as depicted in **Figure 3c**. This constitutes a major challenge in the use of PECL for NIR imaging. To improve the resolution of localized PECL, it is thus necessary to apply a modification of the Si material to minimize its minority carrier lateral diffusion. Ciampi and Gooding showed that the modification of crystalline Si surfaces with amorphous Si thin films (presenting a shorter minority carrier diffusion length)[58–61] improved the resolution in spatially-resolved electrochemistry, however, it was reported that this strategy was not effective for localized PECL.[34] Our group then modified the crystalline planar Si with micropillars,[57] which was determined beneficial for confining holes within the laser area by simulations. Ir layer was homogenously deposited on the top of the Si/SiO_x pillars and inhomogeneously on the sides/bottom of pillars. The profile of the PECL spot, generated with a NIR laser width of 60 µm had a FWHM of 60 µm, demonstrating that a good resolution can be obtained using our strategy and the appropriated P_{laser}. A NIR image (λ_{exc} = 850 nm, P_{LED} = 8 and 28 mW cm^{-2}), comprising

the logo of CNRS (**Figure 3d**) was then projected to planar Si and Si micropillars. While the image could be made visible on the Si micropillars, no PECL was recorded on planar Si at P_{LED} = 8 mW cm^{-2} and no pattern was observed at P_{LED} = 28 mW cm^{-2}. This experiment demonstrated that the Si micropillars decreased the lateral hole diffusion and significantly improved the resolution for imaging applications.

4.3. Bioimaging and microscopy

With the development of ECL for bioanalysis and the promise of AO-ECL, PECL has been extended to bioimaging applications. The first result concerned single cells observed on an optical epifluorescence microscope with the $[Ru(bpy)_3]^{2+}$-TPrA system.[4] For that, the cells were previously grown on a *n*-Si/SiO_x/Ir MIS photoanode. Before microscopy experiments and according to the type of PECL imaging, the cells were pretreated in two ways: *i*) for positive PECL (see **Section 1.1.**), the cell membrane was biotinylated, labeled with the luminophore linked to a streptavidin (SA@$[Ru(bpy)_3]^{2+}$) and permeabilized by Triton-X 100 for direct observation,[62] as shown in **Figure 3e**; *ii*) for negative PECL (see **Section 1.1.**), the cells were not labeled with an ECL luminophore but with calcein-AM (to be localized on the microscope by FL).[63] The cells were then observed by PECL in a back-illumination configuration using a NIR LED, at λ_{exc} = 1050 nm. The cells labeled with SA@$[Ru(bpy)_3]^{2+}$ appeared by positive PECL (**Figure 3f**) at 0.8 V within a solution containing the co-reactant TPrA that can diffuse through the cell membrane and reach the electrode. The cells previously labeled with calcein-AM were imaged by negative PECL by immersing the cells in the electrolyte containing the system $[Ru(bpy)_3]^{2+}$-TPrA. With the local hindrance of the charge transfer by the cell, they appeared dark on a bright background (i.e. bare electrode generating stronger PECL) as in "Chinese shadows". This highlights the benefits of the photovoltage gained in PECL and the possible

further development into AO-ECL bioimaging (see **Section 3.**). However, it should be mentioned that the background in both positive and negative PECL configurations was higher than in the classic ECL imaging approach.

CONCLUSION AND OUTLOOK

The generation of light by classical ECL only requires the application of a potential to the electrode. The absence of any external light source in ECL constitutes a key advantage compared to photo-excitation techniques (e.g. FL) because it offers a near-zero background and thus a remarkable sensitivity. Therefore, it can be considered counter-intuitive to combine ECL with SC photoelectrochemistry, where illumination is required. However, combining both fields opens new perspectives to ECL and SC photoelectrochemistry.[64] Indeed, the illumination of the depleted SC interface brings extra energy to the system, which can be nicely exploited to develop novel forms of ECL: PECL and AO-ECL. Therefore, it adds a new dimension to ECL and considerably enriches the ECL toolbox because it now enables variation of a new light stimulus and not only of the emitted ECL light. In other words, in PECL, the electrode acts simultaneously as a light absorber and a light emitter. PECL has undergone considerable development, this has been demonstrated by the considerable increase of the PECL stability using a Si-based MIS photoanode. Photoelectrochemical energy conversion is a very active field of research, any new improvement in photoelectrode efficiency and stability will be beneficial to PECL, thus we predict that new advances will be reached soon. By selecting the appropriate SC material and the luminophore, PECL has been thus demonstrated in two configurations: upconversion and downconversion. In the upconversion form, a shift up to 600 nm between both wavelengths has been reported in aqueous media. This is an important parameter because it allows separating both optical signals and performing microscopy experiments. In addition, both

frontside and backside configurations have been reported in PECL; this latter one allows operating under completely dark conditions and thus restores the ultrasensitive detection of ECL with a near-zero background.

Other appealing characteristics of SC photoelectrochemistry are the photovoltage generation and localized light stimuli. Indeed, the onset potentials generating ECL can be shifted to unprecedented low values depending on the photovoltage provided by the SC material under illumination. But, we should mention that other electrochemical reactions, that could potentially interfere with the measurement of the current (less probably with the ECL signal), are also subject to a potential shift as well in PECL. Photo-addressing specific sites of the electrode allowed precise spatiotemporal control over the ECL generation. This could be particularly interesting for imaging and analytical applications. In addition, PECL can play an important role in the understanding and optimization of materials because it allows imaging of the charge transfer reactivity of a photoactive SC-based material down to the nanoscale, something that was hard to perform until now. Because it allows the visualization of photogenerated charge transfer with different reactivity or inhomogeneous charge carrier dynamics, as future trends in PECL, we can envision that SC photoelectrocatalysts and photocatalysts will be studied by PECL microscopy to identify active sites. In addition, PECL should also be beneficial to understand local degradation mechanisms. Indeed, PECL imaging provides a 2D view of the local reactivity and it can help to solve current challenges in SC photoelectrochemistry and photocatalysis.

The combination of ECL and photoelectrochemistry at SC opened unexplored opportunities for both fields. Several AO-ECL systems have been reported where the external light (even sunlight) powered the monolithic devices generating ECL light.[47] However, it is important to notice that the photovoltage provided by the junctions has to be high enough not only to trigger the ECL

reactions but also the counter-reaction. Considering this aspect, some similarities exist conceptually with bipolar electrochemistry.[39] AO–ECL constitutes the simplest experimental ECL configuration reported so far because it is easily activated remotely by light and it does not require any electrical power source, electrical connections nor the classical 3-electrode setup. AO-ECL has the potential to spread the ECL applications in laboratories by making it easier to use and accessible for non-electrochemists. One limit is that AO-ECL has to be affordable. In that sense, designs that were easily processed from commercially available *pin* Si photodiodes are suitable candidates to generate AO-ECL in miniaturized disposable devices. Undoubtedly, the PECL and AO-ECL techniques offer the opportunity not only to revisit the classical applications of the ECL field, but, more importantly, also to make bridges with other fields such as IR imaging, energy conversion, photocatalysis, and with different light conversion schemes. We therefore expect that PECL, AO-ECL, and its future forms will undergo rapid further development shortly and lead to promising new (bio)sensing, imaging applications, and be beneficial in energy research.

AUTHOR INFORMATION

Corresponding Authors

* gabriel.loget@cnrs.fr

* sojic@u-bordeaux.fr

Author Contributions

The manuscript was written through the contributions of all authors. All authors have approved the final version of the manuscript.

Funding Sources

This work was funded by ANR (LiCORN, ANR-20-CE29-0006).

Conflict of interest statement

The authors declare no competing financial interest.

Biographies

Yiran Zhao

Yiran Zhao received her Master degree in Chemical Engineering at the École Nationale Supérieure de Chimie de Rennes (France) in 2019 and Ph.D. degree in Physical Chemistry from the University of Rennes (France) in 2023 under the supervision of Dr. Gabriel Loget. She worked on photoinduced electrochemiluminescence at semiconductor electrodes during her PhD research. She will start her postdoc on overall water splitting at Domen-Hisatomi Laboratory in Shinshu University (Japan) from September 2024.

Julie Descamps

Julie Descamps received her BS in Chemistry from the University of Angers in 2018 and joined in 2019 the company Photonis as a project manager. She completed a Ph.D. in Physical Chemistry at Bordeaux University at the Institut des Sciences Moléculaires with Prof. Neso Sojic in 2024. Her research focused on developing analytical strategies based on ECL for imaging and detection. She currently works as a postdoctoral researcher in electrochemistry for CO_2 capture with the ESPCI and Total Energies.

Yoan Léger

Yoan Léger obtained a Ph.D. in Physics at Université Joseph Fourier in Grenoble in 2007 on the spectroscopy of individual II-VI magnetic quantum dots and the detection of single spin states. He then joined Prof. B. Deveaud's group in EPFL to work on exciton-polariton quantum fluids in III-V semiconductor microcavities. In 2012, He became a CNRS researcher at Institut FOTON in Rennes. His current activities focus on nonlinear phenomena in integrated III-V photonics on silicon and semiconductor photo-electrochemistry.

Neso Sojic

Neso Sojic received his Ph.D. in electrochemistry from the Université Pierre et Marie Curie (Paris, France). After postdoctoral studies at the University of Texas at Dallas, he joined the faculty at the University of Bordeaux (France). His main research interests are in analytical electrochemistry, electrochemiluminescence, bioelectrochemistry, microscopy and fiber optic sensors.

Gabriel Loget

After his Ph.D. and postdocs, Gabriel Loget joined the CNRS in 2015 as a researcher at the Institut des Sciences Chimiques de Rennes (France) where he received his habilitation in 2020. In 2024, he moved to the Institut des Sciences Moléculaires in Bordeaux (France). His research interests combine electrochemistry and material sciences for energy and light conversion.

REFERENCES

(1) Zhao, Y.; Yu, J.; Xu, G.; Sojic, N.; Loget, G. Photoinduced Electrochemiluminescence at Silicon Electrodes in Water. *J. Am. Chem. Soc.* **2019**, *141* (33), 13013–13016.

(2) Zhao, Y.; Descamps, J.; Ababou- Girard, S.; Bergamini, J.; Santinacci, L.; Léger, Y.; Sojic, N.; Loget, G. Metal- Insulator- Semiconductor Anodes for Ultrastable and Site- Selective Upconversion Photoinduced Electrochemiluminescence. *Angew. Chem. Int. Ed.* **2022**, *61* (20), e202201865.

(3) Zhao, Y.; Descamps, J.; Al Hoda Al Bast, N.; Duque, M.; Esteve, J.; Sepulveda, B.; Loget, G.; Sojic, N. All-Optical Electrochemiluminescence. *J. Am. Chem. Soc.* **2023**, *145* (31), 17420–17426.

(4) Descamps, J.; Zhao, Y.; Goudeau, B.; Manojlovic, D.; Loget, G.; Sojic, N. Infrared Photoinduced Electrochemiluminescence Microscopy of Single Cells. *Chem. Sci.* **2024**, *15* (6), 2055–2061.
(5) Bard, A. J. *Electrogenerated Chemiluminescence*; M. Dekker: New York, 2004.
(6) Liu, Z.; Qi, W.; Xu, G. Recent Advances in Electrochemiluminescence. *Chem. Soc. Rev.* **2015**, *44* (10), 3117–3142.
(7) Rebeccani, S.; Zanut, A.; Santo, C. I.; Valenti, G.; Paolucci, F. A Guide Inside Electrochemiluminescent Microscopy Mechanisms for Analytical Performance Improvement. *Anal. Chem.* **2022**, *94* (1), 336–348.
(8) Zanut, A.; Fiorani, A.; Canola, S.; Saito, T.; Ziebart, N.; Rapino, S.; Rebeccani, S.; Barbon, A.; Irie, T.; Josel, H.-P.; Negri, F.; Marcaccio, M.; Windfuhr, M.; Imai, K.; Valenti, G.; Paolucci, F. Insights into the Mechanism of Coreactant Electrochemiluminescence Facilitating Enhanced Bioanalytical Performance. *Nat. Commun.* **2020**, *11* (1), 2668.
(9) Yang, X.; Hang, J.; Qu, W.; Wang, Y.; Wang, L.; Zhou, P.; Ding, H.; Su, B.; Lei, J.; Guo, W.; Dai, Z. Gold Microbeads Enabled Proximity Electrochemiluminescence for Highly Sensitive and Size-Encoded Multiplex Immunoassays. *J. Am. Chem. Soc.* **2023**, *145* (29), 16026–16036.
(10) Dong, J.; Lu, Y.; Xu, Y.; Chen, F.; Yang, J.; Chen, Y.; Feng, J. Direct Imaging of Single-Molecule Electrochemical Reactions in Solution. *Nature* **2021**, *596* (7871), 244–249.
(11) Chen, M.-M.; Xu, C.-H.; Zhao, W.; Chen, H.-Y.; Xu, J.-J. Super-Resolution Electrogenerated Chemiluminescence Microscopy for Single-Nanocatalyst Imaging. *J. Am. Chem. Soc.* **2021**, *143* (44), 18511–18518.
(12) Ma, C.; Cao, Y.; Gou, X.; Zhu, J.-J. Recent Progress in Electrochemiluminescence Sensing and Imaging. *Anal. Chem.* **2020**, *92* (1), 431–454.
(13) Zhang, J.; Arbault, S.; Sojic, N.; Jiang, D. Electrochemiluminescence Imaging for Bioanalysis. *Annu. Rev. Anal. Chem.* **2019**, *12* (1), 275–295.
(14) Lu, Y.; Huang, X.; Wang, S.; Li, B.; Liu, B. Nanoconfinement-Enhanced Electrochemiluminescence for *in Situ* Imaging of Single Biomolecules. *ACS Nano* **2023**, *17* (4), 3809–3817.
(15) Ma, C.; Wu, S.; Zhou, Y.; Wei, H.; Zhang, J.; Chen, Z.; Zhu, J.; Lin, Y.; Zhu, W. Bio- Coreactant- Enhanced Electrochemiluminescence Microscopy of Intracellular Structure and Transport. *Angew. Chem. Int. Ed.* **2021**, *133* (9), 4957–4964.
(16) Xu, L.; Li, Y.; Wu, S.; Liu, X.; Su, B. Imaging Latent Fingerprints by Electrochemiluminescence. *Angew. Chem. Int. Ed.* **2012**, *124* (32), 8192–8196.
(17) Becquerel, M. E. Mémoire Sur Les Effets Electriques Produits Sous l'Influence Des Rayons Solaires. *C. R. Acad. Sci.* **1839**, *9*, 561–567.
(18) Fujishima, A.; Honda, K. Electrochemical Photolysis of Water at a Semiconductor Electrode. *Nature* **1972**, *238* (5358), 37–38.
(19) Gerischer, H. Solar Photoelectrolysis with Semiconductor Electrodes. In *Solar Energy Conversion: Solid-State Physics Aspects*; Springer: Berlin, 1979; pp 115–172.
(20) Tan, M. X.; Laibinis, P. E.; Nguyen, S. T.; Kesselman, J. M.; Stanton, C. E.; Lewis, N. S. Principles and Applications of Semiconductor Photoelectrochemistry. *Prog. Inorg. Chem.* **1994**, *41*, 21–144.
(21) Memming, R. *Semiconductor Electrochemistry*; John Wiley & Sons, 2015.

(22) Ager, J. W.; Shaner, M. R.; Walczak, K. A.; Sharp, I. D.; Ardo, S. Experimental Demonstrations of Spontaneous, Solar-Driven Photoelectrochemical Water Splitting. *Energy Environ. Sci.* **2015**, *8* (10), 2811–2824.
(23) Loget, G. Water Oxidation with Inhomogeneous Metal-Silicon Interfaces. *Curr. Opin. Colloid Interface Sci.* **2019**, *39*, 40–50.
(24) Zhao, Y.; Bouffier, L.; Xu, G.; Loget, G.; Sojic, N. Electrochemiluminescence with Semiconductor (Nano)Materials. *Chem. Sci.* **2022**, *13* (9), 2528–2550.
(25) Laser, D.; Bard, A. J. Semiconductor Electrodes. Photo-Induced Electrogenerated Chemiluminescence and up-Conversion at Semiconductor Electrodes. *Chem. Phys. Lett.* **1975**, *34* (3), 6.
(26) Luttmer, J. D.; Bard, A. J. Electrogenerated Chemiluminescence. *J. Electrochem. Soc.* **1979**, *126* (3), 414–419.
(27) Yu, J.; Saada, H.; Abdallah, R.; Loget, G.; Sojic, N. Luminescence Amplification at $BiVO_4$ Photoanodes by Photoinduced Electrochemiluminescence. *Angew. Chem. Int. Ed.* **2020**, *59* (35), 15157–15160.
(28) Yu, J.; Saada, H.; Sojic, N.; Loget, G. Photoinduced Electrochemiluminescence at Nanostructured Hematite Electrodes. *Electrochim. Acta* **2021**, *381*, 138238.
(29) Zhao, Y.; Yu, J.; Xu, G.; Sojic, N.; Loget, G. Photoinduced Electrochemiluminescence at Silicon Electrodes in Water. *J. Am. Chem. Soc.* **2019**, *141* (33), 13013–13016.
(30) Zhao, Y.; Descamps, J.; Léger, Y.; Santinacci, L.; Zanna, S.; Sojic, N.; Loget, G. Upconversion Photoinduced Electrochemiluminescence of Luminol-H_2O_2 at Si/SiO_x/Ni Photoanodes. *Electrochimica Acta* **2023**, *444*, 142013.
(31) Laser, D.; Bard, A. J. Semiconductor Electrodes. IV. Electrochemical Behavior of n- and p-Type Silicon Electrodes in Acetonitrile Solutions. *J. Phys. Chem.* **1976**, *80* (5), 459–466.
(32) Bae, D.; Seger, B.; Vesborg, P. C. K.; Hansen, O.; Chorkendorff, I. Strategies for Stable Water Splitting via Protected Photoelectrodes. *Chem. Soc. Rev.* **2017**, *46* (7), 1933–1954.
(33) Sun, K.; Shen, S.; Liang, Y.; Burrows, P. E.; Mao, S. S.; Wang, D. Enabling Silicon for Solar-Fuel Production. *Chem. Rev.* **2014**, *114* (17), 8662–8719.
(34) Vogel, Y. B.; Darwish, N.; Ciampi, S. Spatiotemporal Control of Electrochemiluminescence Guided by a Visible Light Stimulus. *Cell Rep. Phys. Sci.* **2020**, *1* (7), 100107.
(35) Pourbaix, M. *Atlas of Electrochemical Equilibria in Aqueous Solutions*; National Association of Corrosion Engineers, 1974.
(36) Tung, R. T. The Physics and Chemistry of the Schottky Barrier Height. *Appl. Phys. Rev.* **2014**, *1* (1), 011304.
(37) Lin, F.; Boettcher, S. W. Adaptive Semiconductor/Electrocatalyst Junctions in Water-Splitting Photoanodes. *Nat. Mater.* **2014**, *13* (1), 81–86.
(38) Descamps, J.; Zhao, Y.; Yu, J.; Xu, G.; Léger, Y.; Loget, G.; Sojic, N. Anti-Stokes Photoinduced Electrochemiluminescence at a Photocathode. *Chem. Commun.* **2022**, *58* (47), 6686–6688.
(39) Loget, G.; Zigah, D.; Bouffier, L.; Sojic, N.; Kuhn, A. Bipolar Electrochemistry: From Materials Science to Motion and Beyond. *Acc. Chem. Res.* **2013**, *46* (11), 2513–2523.
(40) Zhao, Y.; Descamps, J.; Le Corre, B.; Léger, Y.; Kuhn, A.; Sojic, N.; Loget, G. Wireless Anti-Stokes Photoinduced Electrochemiluminescence at Closed Semiconducting Bipolar Electrodes. *J. Phys. Chem. Lett.* **2022**, *13* (24), 5538–5544.

(41) Prévot, M. S.; Sivula, K. Photoelectrochemical Tandem Cells for Solar Water Splitting. *J. Phys. Chem. C* **2013**, *117* (35), 17879–17893.
(42) Sun, K.; Liu, R.; Chen, Y.; Verlage, E.; Lewis, N. S.; Xiang, C. A Stabilized, Intrinsically Safe, 10% Efficient, Solar- Driven Water- Splitting Cell Incorporating Earth- Abundant Electrocatalysts with Steady- State pH Gradients and Product Separation Enabled by a Bipolar Membrane. *Adv. Energy Mater.* **2016**, *6* (13), 1600379.
(43) Sivula, K.; Van De Krol, R. Semiconducting Materials for Photoelectrochemical Energy Conversion. *Nat. Rev. Mater.* **2016**, *1* (2), 15010.
(44) Wang, Y.; Schwartz, J.; Gim, J.; Hovden, R.; Mi, Z. Stable Unassisted Solar Water Splitting on Semiconductor Photocathodes Protected by Multifunctional GaN Nanostructures. *ACS Energy Lett.* **2019**, *4* (7), 1541–1548.
(45) Fu, H.-C.; Varadhan, P.; Lin, C.-H.; He, J.-H. Spontaneous Solar Water Splitting with Decoupling of Light Absorption and Electrocatalysis Using Silicon Back-Buried Junction. *Nat. Commun.* **2020**, *11* (1), 3930.
(46) Zhou, P.; Navid, I. A.; Ma, Y.; Xiao, Y.; Wang, P.; Ye, Z.; Zhou, B.; Sun, K.; Mi, Z. Solar-to-Hydrogen Efficiency of More than 9% in Photocatalytic Water Splitting. *Nature* **2023**, *613*, 66–70.
(47) Zhao, Y.; Léger, Y.; Descamps, J.; Sojic, N.; Loget, G. Off- Grid Electrogenerated Chemiluminescence with Customized p- i- n Photodiodes. *Small* **2024**, *20* (14), 2308023.
(48) Zhao, Y.; Descamps, J.; Sojic, N.; Loget, G. All-Optical Electrochemiluminescence at Metal-Insulator-Semiconductor Diodes. *J. Phys. Chem. Lett.* **2024**, *15* (1), 148–155.
(49) Katsounaros, I.; Schneider, W. B.; Meier, J. C.; Benedikt, U.; Biedermann, P. U.; Auer, A. A.; Mayrhofer, K. J. J. Hydrogen Peroxide Electrochemistry on Platinum: Towards Understanding the Oxygen Reduction Reaction Mechanism. *Phys. Chem. Chem. Phys.* **2012**, *14* (20), 7384.
(50) Garcia-Segura, S.; Centellas, F.; Brillas, E. Unprecedented Electrochemiluminescence of Luminol on a Boron-Doped Diamond Thin-Film Anode. Enhancement by Electrogenerated Superoxide Radical Anion. *J. Phys. Chem. C* **2012**, *116* (29), 15500–15504.
(51) Valenti, G.; Fiorani, A.; Li, H.; Sojic, N.; Paolucci, F. Essential Role of Electrode Materials in Electrochemiluminescence Applications. *ChemElectroChem* **2016**, *3* (12), 1990–1997.
(52) Zhang, L.; Liu, J.; Lan, Y.-Q. Hetero-Motif Molecular Junction Photocatalysts: A New Frontier in Artificial Photosynthesis. *Acc. Chem. Res.* **2024**, *57* (6), 870–883.
(53) Laskowski, F. A. L.; Oener, S. Z.; Nellist, M. R.; Gordon, A. M.; Bain, D. C.; Fehrs, J. L.; Boettcher, S. W. Nanoscale Semiconductor/Catalyst Interfaces in Photoelectrochemistry. *Nat. Mater.* **2020**, *19* (1), 69–76.
(54) Liu, T.; Pan, Z.; Vequizo, J. J. M.; Kato, K.; Wu, B.; Yamakata, A.; Katayama, K.; Chen, B.; Chu, C.; Domen, K. Overall Photosynthesis of H2O2 by an Inorganic Semiconductor. *Nat. Commun.* **2022**, *13* (1), 1034.
(55) Descamps, J.; Zhao, Y.; Le-Pouliquen, J.; Goudeau, B.; Garrigue, P.; Tavernier, K.; Léger, Y.; Loget, G.; Sojic, N. Local Reactivity of Metal–Insulator–Semiconductor Photoanodes Imaged by Photoinduced Electrochemiluminescence Microscopy. *Chem. Commun.* **2023**, *59* (82), 12262–12265.
(56) Xue, J.-W.; Xu, C.-H.; Zhao, W.; Chen, H.-Y.; Xu, J.-J. Photoinduced Electrogenerated Chemiluminescence Imaging of Plasmonic Photoelectrochemistry at Single Nanocatalysts. *Nano Lett.* **2023**, *23* (10), 4572–4578.

(57) Zhao, Y.; Sépulveda, B.; Descamps, J.; Faye, F.; Duque, M.; Esteve, J.; Santinacci, L.; Sojic, N.; Loget, G.; Léger, Y. Near-IR Photoinduced Electrochemiluminescence Imaging with Structured Silicon Photoanodes. *ACS Appl. Mater. Interfaces* **2024**, *16* (9), 11722–11729.
(58) Vogel, Y. B.; Gooding, J. J.; Ciampi, S. Light-Addressable Electrochemistry at Semiconductor Electrodes: Redox Imaging, Mask-Free Lithography and Spatially Resolved Chemical and Biological Sensing. *Chem. Soc. Rev.* **2019**, *48* (14), 3723–3739.
(59) Vogel, Y. B.; Gonçales, V. R.; Al- Obaidi, L.; Gooding, J. J.; Darwish, N.; Ciampi, S. Nanocrystal Inks: Photoelectrochemical Printing of Cu_2O Nanocrystals on Silicon with 2D Control on Polyhedral Shapes. *Adv. Funct. Mater.* **2018**, *28* (51), 1804791.
(60) Lim, S. Y.; Kim, Y.-R.; Ha, K.; Lee, J.-K.; Lee, J. G.; Jang, W.; Lee, J.-Y.; Bae, J. H.; Chung, T. D. Light-Guided Electrodeposition of Non-Noble Catalyst Patterns for Photoelectrochemical Hydrogen Evolution. *Energy Environ. Sci.* **2015**, *8* (12), 3654–3662.
(61) Suzurikawa, J.; Nakao, M.; Kanzaki, R.; Takahashi, H. Microscale pH Gradient Generation by Electrolysis on a Light-Addressable Planar Electrode. *Sens. Actuators B: Chem.* **2010**, *149* (1), 205–211.
(62) Voci, S.; Goudeau, B.; Valenti, G.; Lesch, A.; Jović, M.; Rapino, S.; Paolucci, F.; Arbault, S.; Sojic, N. Surface-Confined Electrochemiluminescence Microscopy of Cell Membranes. *J. Am. Chem. Soc.* **2018**, *140* (44), 14753–14760.
(63) Descamps, J.; Colin, C.; Tessier, G.; Arbault, S.; Sojic, N. Ultrasensitive Imaging of Cells and Sub- Cellular Entities by Electrochemiluminescence. *Angew. Chem. Int. Ed.* **2023**, *135* (16), e202218574.
(64) Zhao, Y.; Yu, J.; Yu, Bergamini, J.-F.; Léger, Y.; Sojic, N.; Loget, G. Photoelectrochemistry at Semiconductor/liquid Interfaces Triggered by Electrochemiluminescence. *Cell Rep. Phys. Sci.* **2021**, 2, 100670.